Environmental Science and Pollution Research (2020) 27:34541–34556
https://doi.org/10.1007/s11356-020-09462-0

RESEARCH ARTICLE

Poly(amidoxime) ligand derived from waste palm fiber for the removal of heavy metals from electroplating wastewater

Md Lutfor Rahman[1] · Choong Jian Fui[1] · Mohd Sani Sarjadi[1] · Sazmal E. Arshad[1] · Baba Musta[1] · Mohd Harun Abdullah[1] · Shaheen M. Sarkar[2] · Emmet J. O'Reilly[2]

Received: 21 September 2019 / Accepted: 26 May 2020 / Published online: 17 June 2020

Abstract

A waste material known as palm oil empty fruit bunch (EFB) is used as a source of cellulose for the development of polymeric materials for the removal of metal ions from industrial wastewater. A poly(acrylonitrile)-grafted palm cellulose copolymer was synthesized by a conventional free radical initiating process followed by synthesis of a poly(amidoxime) ligand by oximation reaction. The resulting products were characterized by FT-IR, FE-SEM, EDX, TGA, DSC, and XPS. The poly(amidoxime) ligand was used to coordinate with and extract a series of transition metal ions from water samples. The binding capacity (*qe*) of the ligand with the metal ions such as copper, iron, cobalt, nickel, and lead were 260, 210, 168, 172, and 272 mg g^{-1}, respectively at pH 6. The adsorption process followed the pseudo-first-order kinetic model ($R^2 > 0.99$) and as well as the Freundlich isotherm model ($R^2 > 0.99$) indicating the occurrence of a multi-layer adsorption process in the amidoxime ligand adsorbent. Results from reusability studies show that the ligand can be recycled for at least 10 cycles without any significant losses to its initial adsorption capacity. The synthesized polymeric ligand was shown to absorb heavy metals from electroplating wastewater with up to 95% efficiency.

Keywords Palm cellulose · Acrylonitrile (AN) · Amidoxime · Adsorption · Heavy metals · Electroplate-wastewater

Introduction

Increased industrialization has improved the quality of life for much of the world's population; however, it has also led to increased environmental issues including melting of the ice caps, increased environmental pollutants, and freshwater contamination (Jacob et al. 2018). Of particular concern is the environmental effect of heavy metals as they have been shown to negatively influence physiological processes in biological systems (Wu et al. 2018). Untreated sewage is the primary source of heavy metal contamination in water supplies. As such countries are increasingly introducing regulations and environmental acts highlighting the need to remove toxic metals present in the effluents prior to release into water supplies. The central nervous system (CNS) is the main target of lead poisoning (Wani et al. 2015). The early symptoms of the effect of lead exposure on the central nervous system are severe headaches and loss of memory. Acute exposure to lead leads to brain damage, kidney damage, and long-term CNS damage, while chronic exposure may cause effects on the blood, central nervous system, kidney, and blood pressure (Wani et al. 2015). Excessive levels of copper in the human body can result in anemia, immunotoxicity, and liver damage. In addition, high absorption of copper in plant life will reduce the growth of plants and cause physiological damage (Arif et al. 2016). Effective strategies for the removal of toxic metals from wastewater are therefore critical (Hokkanen et al. 2016).

The Environmental Protection Agency (EPA) in association with the World Health Organization (WHO) has recommended minimum discharge limits for toxic metals. (Fu et al. 2014). Current methodologies for the removal of toxic metal ions from industrial sewages include nano-filtration, precipitation, reverse osmosis, coagulation and flocculation, and

Responsible editor: Angeles Blanco

✉ Md Lutfor Rahman
lutfor73@gmail.com

[1] Faculty of Science and Natural Resources, Universiti Malaysia Sabah, 88400 Kota Kinabalu Sabah Malaysia

[2] Department of Chemical Sciences, Bernal Institute, University of Limerick, Limerick Ireland

adsorption (Fu et al. 2014; Rahman et al. 2016a, b; Pan et al. 2018). Adsorption is regarded as the simplest and most effective process of those outlined. It is preferred as it exhibits high selectivity for the pollutant and high retention once captured (Chen et al. 2018; dos Santos Silva et al. 2018; Lin et al. 2018). Typical adsorbents include zeolites, resins, activated carbon, microspheres, and mesoporous materials (Pan et al. 2018). These adsorbents however are often limited low adsorptions capacity and high cost. In addition, difficulty with material regeneration limits their applications and further increases cost. Therefore, there is significant demand for novel adsorbents with high capacity for regeneration to replace conventional adsorbents (Lin et al. 2018). Cellulose-supported adsorbents have attracted much attention as it is a natural polymer and the most abundant polysaccharide in nature (dos Santos Silva et al. 2018). Cellulose is biodegradable, cost-effective, and insoluble in water. In addition, agricultural waste, also known as biomass contains a high amount of lignin, hemicellulose, and cellulose making it readily available (Lin et al. 2018). However, pure cellulose, as an adsorbent, has low adsorption capacity due to the low activity of the hydroxyl group present on the cellulose. Therefore, several active functional groups such as nitrile, carboxyl, amine, sulfur, and the amino groups have been introduced on the surface of cellulose to increase adsorption capacity (Dwivedi et al. 2014; Liu et al. 2016; Rahman et al. 2016a, b; Rahman et al. 2017; dos Santos Silva et al. 2018).

In this work, a waste product known as palm oil empty fruit bunch (EFB) was chemically modified to act as a low-cost adsorbent for heavy metals. EFB was treated in alkaline media for delignification followed by chemical modification with acrylonitrile (AN). The cellulose-g-polyacrylonitrile (PAN) was then converted into the poly(amidoxime) ligand. After structural and morphological characterization, the adsorption capacity of the palm cellulose-based poly(amidoxime) for metal ions was evaluated at different pH, contact times, and metal ion concentrations including electroplating wastewater (the experimental section is presented in the ESI).

Results and discussion

We have synthesized an effective, reusable, and highly stable polymeric adsorbent for removal of toxic metals ions from industrial sewage based on poly(amidoxime) derived from imine chemistries. Imines contain a double bond of carbon-nitrogen with the general structure R1R2C=NR3. Generally, imines are typically formed when the oxygen of a ketone or aldehyde is replaced with a carbon-nitrogen group (NR group). When R3 is a hydroxyl group, imines are referred to as oximes, where R1 is a hydrocarbon chain and R2 can be an additional hydrocarbon (ketoxime) or a hydrogen atom (aldoxime). Amidoxime is a chemical compound consisting of an amide and oxime and has the general RC(NH2) = NOH.

The formation of the compound is due to the substitution of oximes of carboxamide. Since amidoxime was derived from amide of oxime, both have the almost identical structures (Long et al. 2015). Poly(amidoxime) is a polymer of amidoxime. Rahman et al. previously reported the synthesis of poly(amidoxime) from various sources of cellulose and investigated the adsorption properties (Rahman et al. 2016a, b; Pan et al. 2016). Amidoxime is a well-known potential chelating ligand, which can be used as an adsorbent. Syntheses of the amidoxime ligand and intermediate products are shown in Scheme 1.

FT-IR spectroscopy analysis

Figure 1 shows the results from the infrared spectrum for each of the materials used in this study. Spectra of the palm cellulose, palm cellulose-grafted PAN, and the palm cellulose-based poly(amidoxime) ligand are overlaid for comparison. IR stretching and bending peaks belonging to the respective functional groups have changed in the spectrum of the products; however, most of the peaks are retained similar to the cellulose materials. Typically, a sharp and clear nitrile peak indicates that the grafting process was successful from cellulose and acrylonitrile monomer. FT-IR analysis of the palm cellulose, palm-grafted-PAN, and poly(amidoxime) ligand are discussed in detail below.

The spectrum of pure cellulose from the palm fiber (EFB) indicates a broad-ranging absorption peak at 3462 cm^{-1} representing the stretching of a hydroxyl and a peak at 2917 cm^{-1} due to carbon-hydrogen stretching (Fig. 1(a)), which in accordance with the previous study (Pan et al. 2016; Rahman et al. 2016a, b). Absorbed water on the cellulose showed a bending mode of broad band at 1638 cm^{-1}. The absorption bands at 1383 cm^{-1} and 1162 cm^{-1} belong to the bending of the hydroxyl group and extending of C–O group respectively (Rahman et al. 2016a, b). The cyclic six-member ring structure known as pyranose cyclic skeletal structure (C–O–C) on the saccharide cellulose structure shows a significant broadband stretch at 1060 cm^{-1} and a small intense peak at 891 cm^{-1} belonging to the linkage of glycosidic C_1–H distortion with hydroxyl bending. This is a physical identification of α-glycosidic linkage that forms between the repeating units of glucose on the cellulose structure (Pan et al. 2016). The extracted palm-based cellulose in this work was in pure form, not hemicellulose (Lin et al. 2018). The stretch at 1029 cm^{-1} can be attributed to the vibration of the pyranose cyclic skeletal structure which can be in the mirror-like or disproportional form (Hokkanen et al. 2016; Rahman et al. 2016a, b).

The IR absorption spectrum of the palm-based cellulose grafted with acrylonitrile (palm cellulose-grafted PAN) produced a new significant sharp peak at 2244 cm^{-1} due to cyano

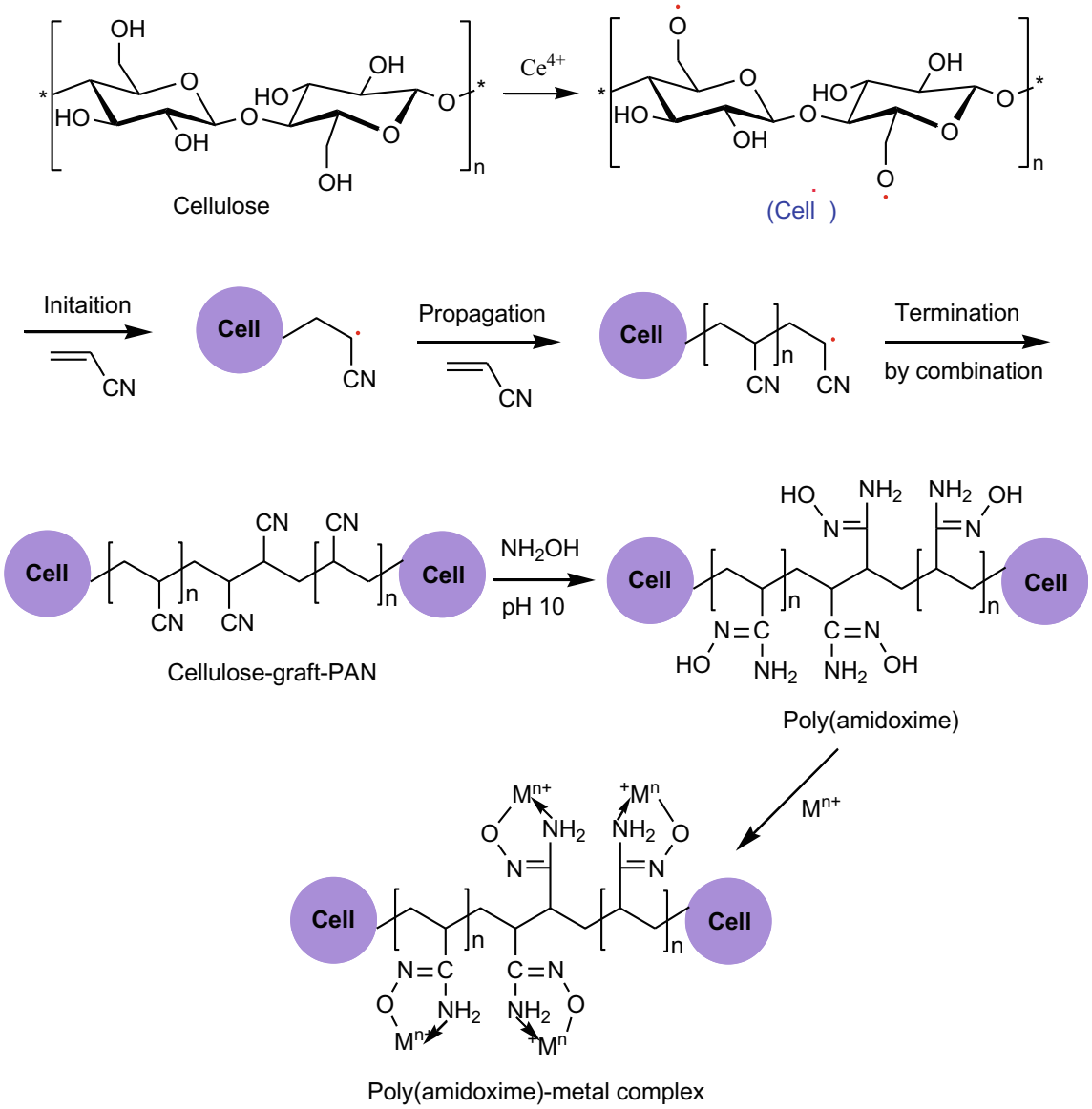

Scheme 1 Graft copolymerization of acrylonitrile onto cellulose (Cell• is a glucose unit) to produce a cellulose-grafted PAN, poly(amidoxime), and poly(amidoxime)-metal complex

functional group (CN) belonging to the acrylonitrile (Fig. 1(b)). The rest of the adsorption peak present in the spectrum of palm cellulose-grafted PAN was retained from the palm cellulose. These peaks are due to the hydroxyl group stretching and bending modes of absorbed water, hydrocarbon symmetry deformations, and hemiacetal cyclic structure skeletal vibrations. Grafting of the cyano group onto the cellulose can be confirmed by the presence of a sharp peak at 2244 cm^{-1}. Cyano functional groups are normally observed in the range of 2500–2000 cm^{-1} for various backbones such as chitosan, cellulose, and silica (Pan et al. 2016, 2018). At the final stage of grafting, the acrylonitrile monomer was grafted onto the cellulose and produced palm cellulose-grafted PAN (Pan et al. 2016).

The new absorption band represents the functional group of amidoxime in the palm cellulose-based ligand and appeared at 1652 cm^{-1} due to the C=N stretch and 1399 cm^{-1} for N–H bending modes (Fig. 1(c)). In addition, a shoulder peak was observed at 3234 cm^{-1} due to both hydroxyl and amide group. The cyano stretching band at 2244 cm^{-1} was replaced by oximes of amide functional groups at 1652 cm^{-1} and 1399 cm^{-1} confirming that all the cyano group present in the PAN was fully converted into oxime of amide functional groups The remaining adsorption peaks present in the spectrum of poly(amidoxime) were retained from palm cellulose and showed the poly(amidoxime) broadening peak at approximately 3100–3500 $cm^{-1}$for N–H stretching and 3300–3700 cm^{-1} for O–H stretching (Pan et al. 2016).

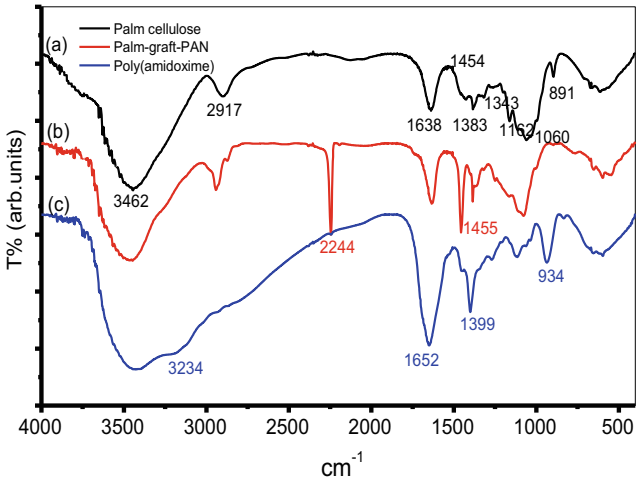

Fig. 1 FT-IR spectra of (a) palm cellulose, (b) cellulose-grafted PAN, and (c) palm cellulose-based poly(amidoxime) ligand

FE-SEM analysis

A gray colored, slightly deformed spherical like morphology was observed for the palm cellulose by the FE-SEM micrograph (Fig. 2a). The poly(acrylonitrile) (PAN)-grafted palm cellulose displayed identifiable grafting on the cellulosic structure as the typical spherical shape of the cellulosic structure was deformed completely, being replaced with a roughened morphology (Fig. 2b). Images show approximately 10–20 spheres accumulated together for the poly(amidoxime) ligand (Fig. 2c). However, after adsorption with copper ions by the poly(amidoxime) ligand, a larger size of the spherical shape is observed with similar accumulation found as shown in Fig. 2d.

Energy dispersive X-ray (EDX) analysis

Figure 3 shows the EDX spectra of poly(amidoxime) ligand after absorbing the copper metal. Upon inspection of the result, it is an evident that the value of copper has been increased post absorption in copper solution with approximately 30.4% of copper being adsorbed on the poly(amidoxime) ligand.

Thermogravimetry analysis

TGA scans of the cellulose, PAN-grafted cellulose, poly(amidoxime) ligand, and poly(amidoxime) ligand-

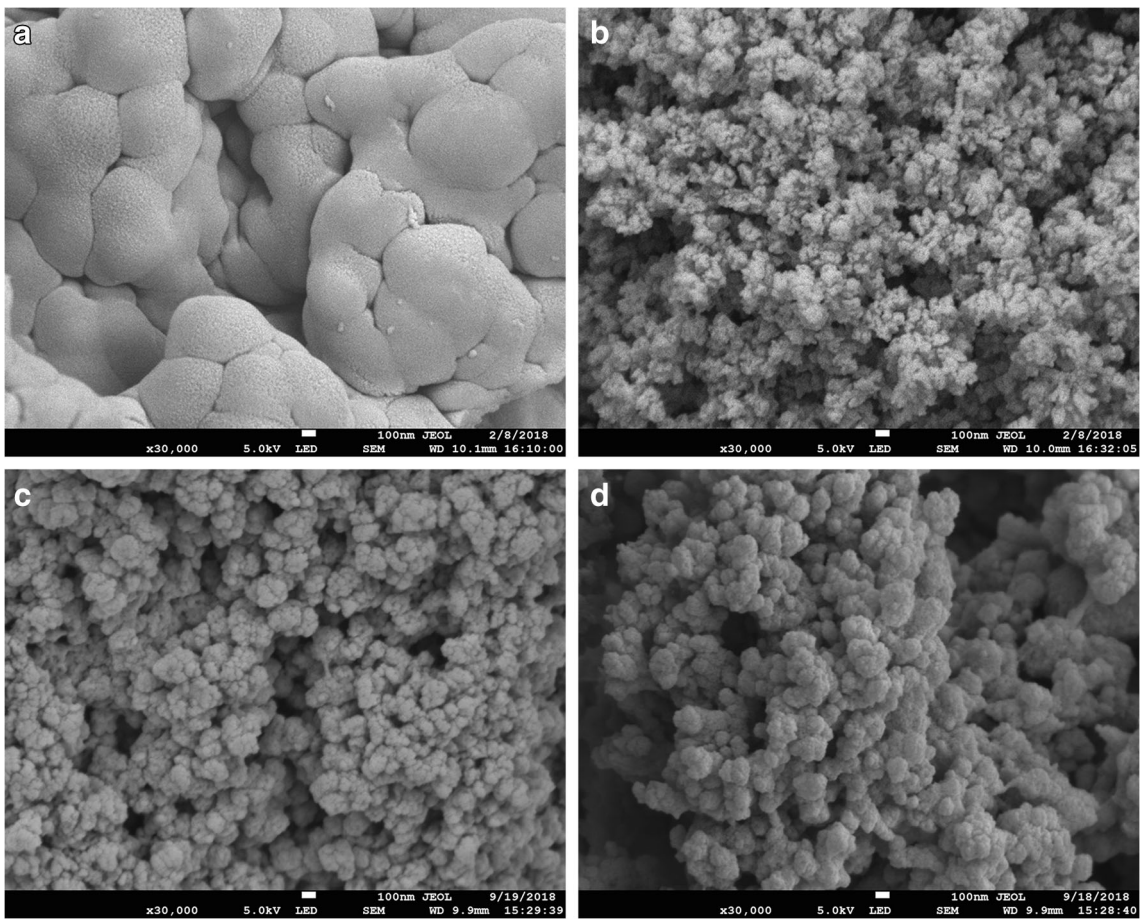

Fig. 2 FE-SEM micrograph of **a** purified palm cellulose, **b** PAN-grafted cellulose, **c** poly(amidoxime) ligand, and **d** poly(amidoxime) ligand after adsorbing copper

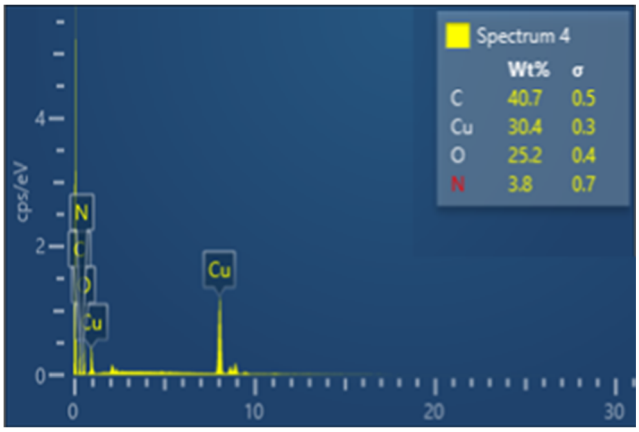

Fig. 3 EDX spectrum of poly(amidoxime)-copper complex

copper complex were performed with heating rate 10 min^{-1} under a nitrogen atmosphere (Mettlar Toledo TGA/DSC +3), and the results of which are presented in Fig. 4. TGA analysis shows that the palm cellulose is of lower thermal stability in the final stage of the experiment (380–800 °C) relative to other samples. The poly(amidoxime) ligand-copper complex is notably more stable showing little degradation. Several changes are observed during the TGA analysis. These include a small weight loss being observed before 120 °C due to the release of water molecules and some volatile organic solvent (methanol, acetone etc.), which are located on the external surface and internal pores and cavities of the cellulose (6%), PAN-grafted cellulose (2%), poly(amidoxime) ligand (9%), and poly(amidoxime) ligand metal complex (8%). The high water content in the poly(amidoxime) ligand confirms that it is a hydrophilic material. The cellulose curve shows that there is a significant weight loss at between 315 and 390 °C (80%) due to the degradation of material such as the hydroxyl group (OH) and CH_2OH function group located on the cellulose surface (Hong et al. 2015). The poly(acrylonitrile)-grafted cellulose showed two stages of weight loss between the temperature range 290–550°C. The first weight loss (38%) occurred at 380°C due to the occurrence of a dehydrogenation reaction and degradation of the grafted functional group (CN). The second stage of the weight loss (17%) occurs between 380 and 550°C and is likely attributed to the degradation of the remaining of poly(acrylonitrile) chain. In both of the stages, the weight loss can be attributed to release the volatile gases such as CO, CO_2, CH_4, NH_4, and HCN. These results are in agreement with several previously reported studies (Salah et al. 2015; Robson et al. 2015; Kiani et al. 2011). The poly(amidoxime) ligand also exhibited two stages of degradation. The first stage degradation occurs between 200 and 300°C (24%) due to the degradation of the amidoxime functional group. They have a cross-section point between PAN-grafted cellulose and poly(amidoxime) ligand at 430 °C. The poly(amidoxime) ligand exhibited increased stability relative to poly(acrylonitrile) until approximately 750 °C. After this, a 60% weight loss was observed for the amidoxime ligand and PAN-grafted cellulose with poly(amidoxime) ligand-copper complex exhibiting weight loss of approximately 55%.

Differential scanning calorimetry analysis

Figure 5 shows a DSC curve where an exothermic thermal event occurs, related to the PAN-grafted cellulose, poly(amidoxime) ligand, and poly(amidoxime) metal complex under inert conditions with heating rate 10 min^{-1} (Mettler Toledo TGA/DSC +3). In general, exothermic reactions on polyacrylonitrile take place due to the cyclization reactions of nitrile groups, dehydrogenation, cross-linking, and oxidative reactions, when treatment is performed at oxidizing atmosphere (Furushima et al. 2014; Ju et al. 2013).

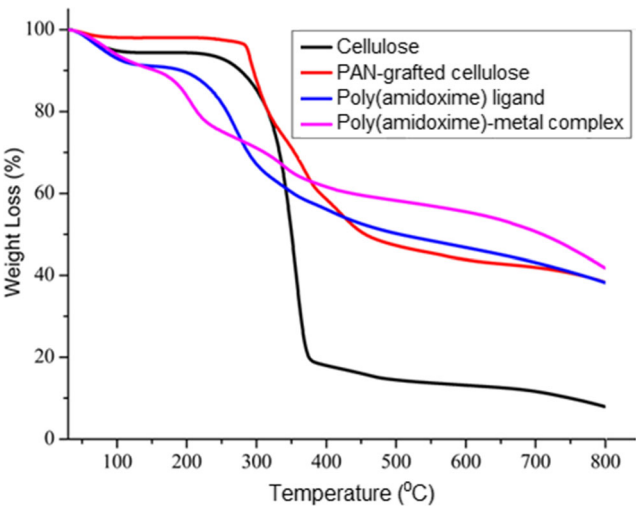

Fig. 4 TGA thermograms of palm-based cellulose, poly(acrylonitrile)-grafted cellulose, poly(amidoxime) ligand, and poly(amidoxime)-copper complex

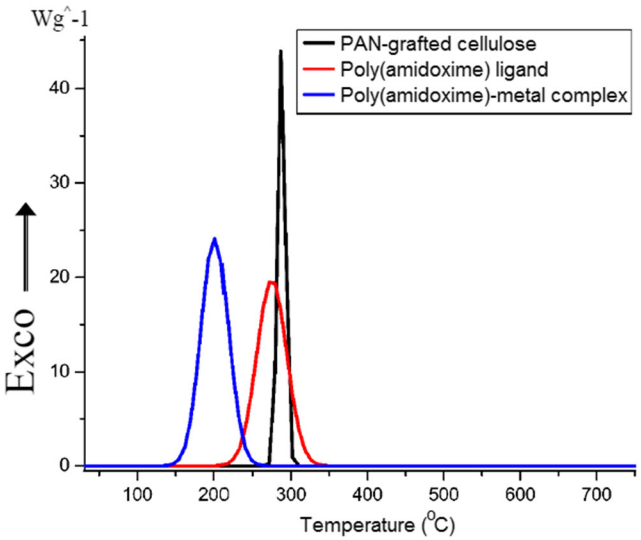

Fig. 5 DSC thermograms of poly(acrylonitrile)-grafted cellulose, poly(amidoxime) ligand, and poly(amidoxime)-copper complex

PAN-grafted cellulose had a significant sharp and narrow peak beginning at 290°C and ending at 314 °C (T_f). The extent of the stabilization event ($\Delta T = T_f - T_i$), under inert condition, is approximately 114°C and releases approximately 2.21 kJ of energy. When the exothermic reaction releases energy in a shorter time interval, the weight loss rate is increased and further responses may become uncontrolled (Robson et al. 2014). This result is in good agreement with previously reported work (Robson et al. 2015; Furushima et al. 2014; Robson et al. 2014). A new exothermic transition was observed at 271°C for poly(amidoxime) with some initial moisture dehydration. The exothermic curve was shifted to the left side due to the amidoximation in the grafted copolymer, thereby confirming formation of the poly(amidoxime) ligand (Lutfor et al. 2000). The exothermic reaction initiated approximately 195°C (T_i), exhibited a medium broad peak at 271°C and finishing at 340 °C (T_f). The extent of the thermal transition ($\Delta T = T_f - T_i$), under inert conditions, is around 145 °C and releases an amount of energy equivalent to 3.33 kJ. The poly(amidoxime) releases high energy compared to the poly(-acrylonitrile). This indicates that poly(amidoxime) ligand is more thermally stable than poly(acrylonitrile). After the adsorption of metal, an exothermic transition is observed at 100 °C (T_i), exhibiting a medium broad peak at 205 °C and finishing at 280 °C (T_f). The extent of the stabilization event ($\Delta T = T_f - T_i$) is around 180 °C and releases an amount of energy equivalent to 3.78 kJ. In conclusion, poly(amidoxime) metal complex is the most stable material as it exhibits a high stabilization event, and it can release a high amount of exothermic energy.

Reaction mechanism

Several studies have been performed on the mechanism by which the grafting reaction occurs using the free radical initiation method (Pan et al. 2016, 2018). An alternative mechanism involving primary OH groups can be considered in this study. This mechanism causes a free radical on the oxygen atom of OH groups of the cellulose unit to form which reacts with the vinyl monomer for the grafting copolymerization reaction (Scheme 1). In this study, palm-based cellulose was grafted with acrylonitrile monomer by a free radical initiation reaction with the ceric ammonium nitrate as an initiator. Due to the ceric salt acting as a one-electron oxidizing agent, it can be used for an oxidative addition reaction of electrophilic radicals. The ceric (IV) ion forms a complex with the OH group on the cellulose. The hydrogen atom on the glucose units in the cellulose was oxidized by the reduction of Ce^{4+} to Ce^{3+}. Then the cellulosic free radicals induced the initiation of grafting by linking to the vinyl group of the acrylonitrile monomer. Furthermore, radical formation resulted in the propagation reaction. At the termination stage, the growing polymer chain of the cellulose-monomer molecules produced in the combination of grafting is shown in Scheme 1, although termination by disproportionality can also occur.

The palm cellulose-grafted PAN has the nitrile group which undergoes functionalization to the amine group. Therefore, the nitrile functional group was the key group which reacted with hydroxylamine to form the chelating ligand poly(amidoxime) adsorbent. The poly(amidoxime) ligand functional group can participate in enhancing the significant binding properties with metal ions. The bidentate poly(amidoxime) chelating ligand contributed five-membered ring complex with metal ions (Scheme 1). Eigen and Tamm proposed the mechanism of chelate formation into a complex structure by the generation of an electrostatic ion pair between the metal and ligand as the first step of the mechanism (Eigen and Tamm 1962). Then the coordination sphere is freed from the water molecule by a ligand at a subsequent step. The second step is slower, and the rate depends on the energy of the metal-ligand bond. This mechanism is referred to the Eigen–Wilkins mechanism (Wilkins 1964; Eigen and Wilkins 1965). The variation of binding capacities is found for the logarithm of kH_2O with the number of d electrons in different metal ions (Helm and Merbach 1999). The rate constant is dependent on the number of d electrons in metal ions (Beccia et al. 2014).

Adsorption study

Effect of pH on the binding of metal ions

The binding capacity of the ligand was investigated with selected metal ions at pH values ranging from 3 to 6 using a batch adsorption technique. After the adsorption reached equilibrium, the adsorbent was removed by filtration, and the remaining solution concentration of metal ions were determined by ICP-OES. The initial and final concentration of the metal ions can be estimated by Eq. 1 (Pan et al. 2016).

$$q_e = \frac{(C_o - C_e)V}{L} \quad (1)$$

where q_e is the binding ability amount of metal ions (mg g^{-1}); C_o and C_e are the beginning concentration of the metal ion solution (ppm) and the final concentration of the metal cation solution, respectively. V is the volume of the metal ion solution (L), and L is the quantity of palm cellulose-based adsorbent (g). There is a significant influence of pH during on the adsorption process by the poly(amidoxime) chelating ligand for the binding of bivalent and trivalent metal cations from the aqueous solution. Five different types of heavy metal were chosen to determine the effect of the pH on the adsorption behavior (Fig. 6). The pH solution is adjusted by acetate buffer (adding acetic acid to the 0.1 M ammonium acetate solution). In this study, the experimental control condition is

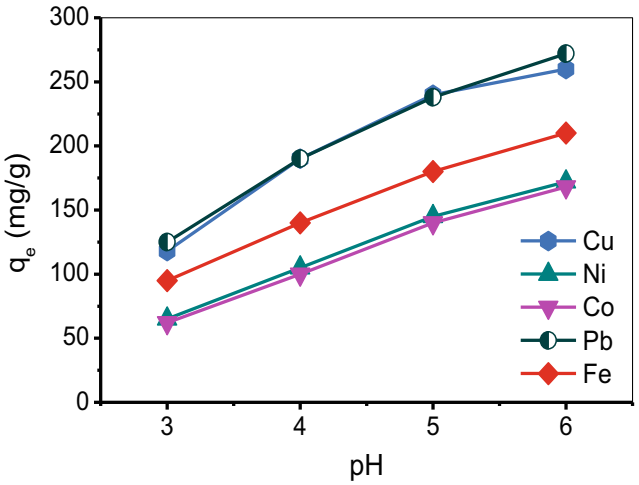

Fig. 6 The influence of pH on the adsorption of bivalent and trivalent metal ions by the synthesized palm-based ligand; experimental variables were 0.5 g of poly(amidoxime) ligand, 15 mL of distilled water, 5 mL of sodium acetate buffer solution at pH 3–6, and 5 mL of 0.2M metal solution and stirred for 2 h

pH 6 in the system for the metal ions to get a consistent result and highly sensitive response by the chelating ligand (Pan et al. 2016; Rahman et al. 2016a, b). The investigation of pH values in the solution above pH 8 was not possible as the divalent or trivalent metal cation can be precipitated out at increasingly alkaline values. Below pH 8, no spontaneous precipitation was observed. Hydroxide precipitation was prevented only by ionic species present in the solution of pH 6 (Ahmad et al. 2015). Figure 6 shows the adsorption characteristics and binding capacities of the synthesized palm-based chelating ligand on the bivalent and trivalent metal ions between pH 3 and 6. It is well-known that the chelating ligand shows favorability toward some metal ions, including lead and copper compared to other three metal cations. The binding capacities for each of the metal ions, Cu^{2+}, Fe^{3+}, Ni^{2+}, Co^{2+}, and Pb^{2+}, are provided in Fig. 6. Results show that the selected metal adsorption by the palm cellulose-based ligand is pH-dependent. The ligand displayed the highest affinity to the lead ions in the pH 6 region, but other metal ions also revealed higher absorption at pH 6 compared to low pH values including copper, cobalt, nickel, and iron. The maximum binding capacities of the poly(amidoxime) ligand for the metals such as Cu^{2+}, Fe^{3+}, Co^{2+}, Ni^{2+}, and Pb^{2+} were 260, 210, 168, 172, and 272 mg g^{-1}. Results show effective complexation of the ligand with respective metal ions in aqueous solutions. As expected, the overall binding capacities of heavy metals by palm cellulose-based ligand increased with increasing pH (up to pH 6). This is due to the amphoteric behavior of the functional group of the ligand molecule of the polymeric adsorbent present (–C(NH_2)=N–OH) (Pan et al. 2016; Rahman et al. 2016a, b). At low pH, more protonation occurs and causes basic $–NH_2$ to become blocked and results in $–NH_3^+$. Besides, as the pH value decreases, the ionization of the –OH will decrease. This result leads to reduced retention of the bivalent and trivalent metal ions on the ligand. This effect is strongly evident in all five selected bivalent and trivalent metal ions. Again, at higher pH, more than pH 8, the protonation of the amino group on the chelation ligand will decrease as the concentration of hydrogen ion (H^+) in aqueous solution decreases (Donia et al. 2014). Therefore, the adsorption character of an amino group on the palm-based poly(amidoxime) for removing metal ions increases. In addition, production of the negative oxygen ion (O^-) increases as the dissociation level of the hydroxyl group (OH^-) increases. This results in an electrostatic association between amidoxime ligand and metal ions. Thus, it leads to a higher binding character toward the bivalent and trivalent toxic metal ions (Donia et al. 2014; Ahmad et al. 2015).

Adsorption kinetics

The initial and final concentration of metal ions was analyzed by ICP-OES. The quantity of the metal ions that was adsorbed by the poly(amidoxime) ligand was calculated using Eq. 2 (Pan et al. 2016):

$$q_t = \frac{(C_o - C_t)V}{L} \quad (2)$$

where q_t is the quantity of metal ions removed by ligand at time t (mg g^{-1}). C_o and C_t are the initial concentration of metal ions (mg L^{-1}) and the final concentration of metal ions, respectively. L represents the mass of polymeric ligand used (g) and V represents the quantity of the metal ion solution (L).

The rate of absorption mechanism of palm cellulose-based ligand in the take-up of bivalent and trivalent ions has been shown to depend on the complexation reaction of the ligand and metal ions rather than ion-exchange or hydrogen bond formation. Therefore, the required contact time between the poly(amidoxime) ligand and the selected metal ions (Cu^{2+}, Fe^{3+}, Ni^{2+}, Co^{2+}, Pb^{2+}) binding was investigated using a set of contact time experiments. The kinetic character on the extraction of bivalent and trivalent ions by the palm cellulose-based ligand with a set of times was investigated and the result was determined by ICP-OES. To fully describe the adsorption kinetics, two types of kinetic model are proposed to adequately interpret and explain the adsorption process. Metal adsorption was show to occur most effectively at pH 6. In order to identify the rate of binding, the most common and straight forward pseudo-first-order kinetic model and pseudo-second-order kinetic model can be evaluated using the analytical data.

Pseudo-first-order kinetic model The pseudo-first-order kinetic equation is used for the elimination of metal ions from the solution. The pseudo-first-order equation is presented by Eq. 3 (Pan et al. 2016; Ayawei et al. 2017):

$$\log(q_e - q_t) = \log q_e - \left(\frac{K_{ads}}{2.303}\right)t \quad (3)$$

where q_e and q_t are the metal ion adsorbed (mg g^{-1}) at end-most and t is the time selected (min), where the rate constant of Lagergren's pseudo-first-order reaction is K_{ads} (min^{-1}). The q_e and K_{ads} values can be calculated from the plot of pseudo-first order by finding the intersection and the gradient of the plot of log ($q_e - q_t$) vs time (Fig. 7) and relative values are present in Table 1. Table 1 also shows the result from the calculation for the ability of binding of five selected bivalent and trivalent cations. Based on this result, the linearity of the plots was shown to be very high and appropriate. The R^2 values of copper, iron, cobalt, lead, and nickel were shown in an accepted range and were 0.999, 0.990, 0.998, 0.997, and 0.998, respectively. The theoretical q_e values of pseudo-first order were obtained from the intercept of the linear plots and theoretical q_e can be compared with the experimental q_e values (Table 1). It was shown that the pseudo-first-order kinetic model fits best to the result when applied to heavy metal adsorption by using palm cellulose-based poly(amidoxime) ligand at varying contact time. The experimental q_e values were shown to be not much different from the corresponding theoretical values. Owing to the high and good linearity of the plots obtained and experimental values of q_e, the study of the adsorption of metal ions by the palm cellulose-based poly(amidoxime) ligand followed the pseudo-first-order kinetic model pathway.

Pseudo-second-order kinetic model The pseudo-second-order kinetic model is used to express the adsorption rate's association with the different adsorption abilities with varying contact time. This pseudo-second-order kinetic model can be expressed by Eq. 4 (Ayawei et al. 2017):

$$\frac{t}{q_t} = \frac{1}{k_2 q_e^2} + \frac{t}{q_e} \quad (4)$$

where k_2 represents the rate constant of the second-order sorption (g mg^{-1} min^{-1}), q_t is the amount of metals eliminated (mg g^{-1}) at any time, and the q_e is the quantity of the metal ions adsorbed (mg g^{-1}) at equilibrium. The values of k_2 and q_e can be estimated from the graph of t/q_t versus time (Fig. 8) and the corresponding values are shown in Table 2. Table 2 also shows the result from the calculation for the capacity character of five selected toxic metal ions. Based on the calculated result, a significant difference was found between the parameter presented by pseudo-first order and pseudo-second order (Tables 1 and 2). The data in Table 2 also shows the high and consistent value of the correlation coefficient (R^2) for the pseudo-second order, but there are significant differences between the theoretical q_e value and experimental data. The values of R^2 for the iron, lead, copper, zinc, and cobalt were

Table 1 Adsorption rate specification of the pseudo-first-order model for transition metals by the poly(amidoxime) chelating ligand

Adsorbate	Pseudo-first order			Experimental
	q_e (mg g^{-1})	K_1 (min^{-1})	R^2	q_m (mg g^{-1})
Cu	251	0.0183	0.999	260
Fe	193	0.0139	0.990	210
Co	164	0.0128	0.998	172
Pb	268	0.0175	0.997	272
Ni	166	0.0132	0.998	168

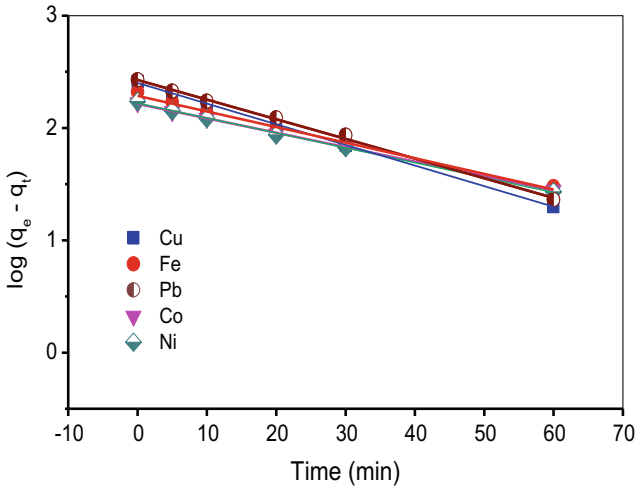

Fig. 7 The kinetic character of Lagergren's pseudo-first order on the adsorption of metal ions by the synthesized palm-based ligand; experimental variables were 0.5 g of poly(amidoxime), 15 mL of distilled water, 5 mL of pH 6 buffer solution, and 5 mL of 0.2 M synthetic metal ion solution and stirred for 2 h

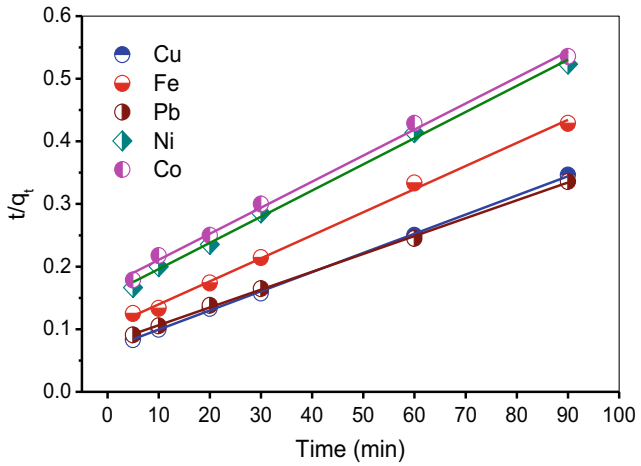

Fig. 8 The kinetic character of pseudo-second order on the adsorption of metal cations by the synthesized ligand; experimental variables were 0.5 g of poly(amidoxime), 15 mL of distilled water, 5 mL of pH 6 buffer solution, and 5 mL of 0.2 M synthetic metal cation solution and stirred for 2 h

Table 2 Adsorption rates specification of the pseudo-second-order model for transition metals by the poly(amidoxime) chelating ligand

Adsorbate	Pseudo-second order			Experimental
	q_e (mg g^{-1})	K_2 (g mg^{-1} min^{-1}) × 10^{-3}	R^2	q_m (mg g^{-1})
Cu	333	0.0686	0.999	260
Fe	277	0.1027	0.996	210
Co	244	0.1693	0.995	172
Pb	357	0.0778	0.999	272
Ni	243	0.1544	0.996	168

all more than 0.99 and near to 1. Owing to that, the R^2 value is high for all metal ions, but the numerate q_e values had discrepancies with the experimental data. Therefore, the adsorption process followed the pseudo-second-order pathway the least, and the chemical process of the adsorption mechanism was by the valance forces through the transferring or exchanging electrons in association with the polymeric chelating ligand and the metal ions (Donia et al. 2014; Pan et al. 2016).

Sorption isotherm

To determine the sorption behavior, the conventional batch method was used to conduct the adsorption experiment with different concentrations of metal ion solution (250 to 4000 ppm). After equilibrium, the palm cellulose-supported polymer was separated, and the concentrations of metal ions were determined by ICP-OES. The result was calculated using Eq. 1 (Pan et al. 2016). Different concentrations of heavy metals contained in aqueous solution on the binding character and the sorption isotherm studies were necessary owing to verify that the palm cellulose-supported adsorbent can be a good candidate in low-concentration heavy metal-containing solution. The sorption isotherm study was performed using the prepared adsorbent with the selected toxic metal ions (Cu^{2+}, Fe^{3+}, Ni^{2+}, Co^{2+}, and Pb^{2+}) in which variouas metal ions concentration were used from 250 - 4000 ppm, while other parameters such as amount of ligand used, pH of the buffer, shaking time, and shaking speed were set as constant values. The outcome from the experiment implies that the potential of the binding by synthesizing ligand was increased as the initial concentration of bi- and trivalent metal ions used increases. The binding capacity of Cu^{2+}, Fe^{3+}, Ni^{2+}, Co^{2+}, and Pb^{2+} is steadily raised from 250 ppm while highest capacity attained at 4000 ppm, as shown in Fig. 9.

Nonlinear forms of Langmuir isotherm model

The Langmuir isotherm theory is the most fundamental theory in adsorption since 1918. The Langmuir isotherm theory is expanded to describe the saturated monolayer on the homogeneous and flat surface of adsorbent at equilibrium states (migration restricted, constant energy, and rate of adsorption) (Ahmadpour et al. 2014). This model is applied to the gases adsorbed on the solid surface. The Langmuir theory is a semi-empirical isotherm and it is derived based on the statistical thermodynamics (Jang et al. 2018). This theory was used to describe the rate of accumulation of molecules at the flat surface at zero equilibrium. The assumptions of the Langmuir isotherm theory are (a) all the adsorption sites are energetically identical (homogeneous surface), (b) the adsorption on the flat surface is localized (monolayer adsorption), (c) each site can favor one molecular or atom, and (d) all adsorption occurs in the same mechanism (Silva et al. 2013). The nonlinear Langmuir adsorption isotherm expression is shown in Eq. 5 (Pan et al. 2016).

$$q_e = \frac{q_{max} K_L C_e}{1 + K_L C_e} \quad (5)$$

where q_e (mg g^{-1}) is the adsorption capacity of metal ions on the cellulose-based adsorbent, C_e (mg L^{-1}) is the concentration of metal ions in aqueous solution, and q_{max} (mg g^{-1}) and K_L (L g^{-1}) are the maximum capacity and Langmuir adsorption constants, respectively.

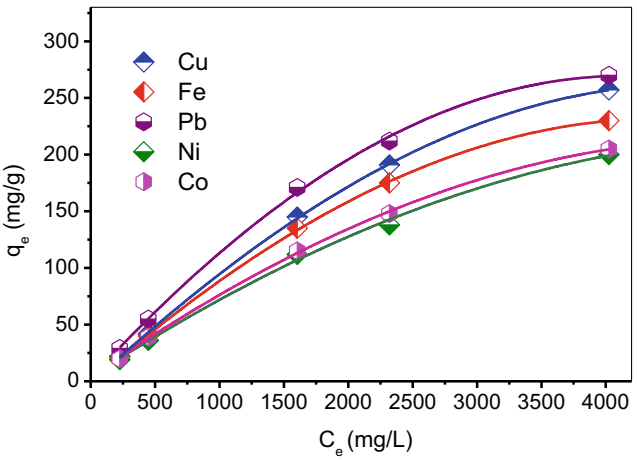

Fig. 9 The effect of initial concentration of metal ions in solution on the adsorption of metal ions by synthesized palm-based ligand; experimental variables were 0.5 g of poly(amidoxime), 15 mL of distilled water, 5 mL of pH 6 buffer solution, and 5 mL of 0.2 M synthetic metal ion solution and stirred for 2 h

The parameters were obtained from the linear plot of the q_e versus C_e (Fig. 9). The parameters were evaluated by nonlinear regression method using the Origin 8.0 Software. Figure 9 shows Langmuir adsorption isotherms of the adsorbents by nonlinear analysis and the isotherm parameters are shown in Table 3. The values of maximum adsorption capacity determined using the Langmuir model were 256, 229, 204, 269, and 199 mg g^{-1} of Cu, Fe, Co, Pb, and Ni, respectively. Most of metal ion adsorption values obtained by the Langmuir model are close to the experimental q_e, which indicates that the nonlinear modeling of Langmuir for the adsorption system is in good agreement.

Linear forms of the isotherm models

The general isotherm model, linear forms of Langmuir, and the Freundlich isotherm are frequently used to deeply explain the isotherm specification for the adsorption system. The linear form of two isotherm models is conventionally introduced because both equations had been simplified and easy to understand (Pan et al. 2016).

The linear Langmuir adsorption isotherm expression is present in Eq. 6 (Pan et al. 2016).

$$\frac{C_e}{q_e} = \frac{1}{q_{max} K_L} + \frac{C_e}{q_{max}} \quad (6)$$

The linear Langmuir isotherm theory is widely used to investigate the isotherm parameters or the best value for the adsorption process. The Langmuir isotherm theory also can be presented in terms of a dimensionless parameter. The result of the Langmuir isotherm model in a dimensionless equation defines the tendency of the isotherm to be unfavorable ($R_L > 1$), linear ($R_L = 1$), favorable ($0 < R_L < 1$), and irreversible ($R_L = 0$) and defines the affinity between the adsorbate and adsorbent (Pan et al. 2016; Jang et al. 2018).

The resultant data summarized that the bivalent and trivalent toxic metal ions eliminated by synthesized palm cellulose-based polymeric ligand did not fit well with the Langmuir isotherm model (Fig. 10). Only the R^2 value of lead

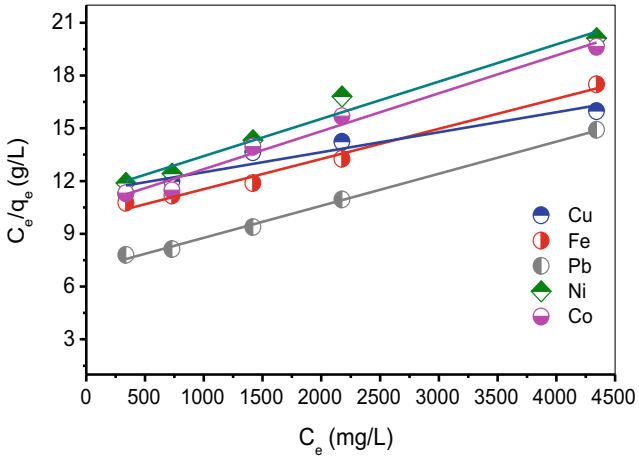

Fig. 10 Langmuir isotherm curves obtained by linear fitting on the adsorption of metal ions by the synthesized palm-based ligand; experimental variables were 0.5 palm-based modified ligand, 15 mL of distilled water, 5 mL of pH 6 buffer solution, and 5 mL of 0.2 M synthetic metal ion solution and stirred for 2 h

(0.996) was shown to be in a good and well-accepted range. The rest of the metal ions show the inadequacy of R^2 values which are all below 0.990. The theoretical q_m values of Langmuir model obtained from the intercept of the linear plots were also compared with the experimental q_e values. The calculated results from the maximum binding ability (q_m) and the sorption coefficient K_L is presented in Table 4. The maximum sorption capacity was derived from the linear plot of Langmuir isotherm but is significantly different from the experiment data q_e. Therefore, it can be concluded that the adsorption study of the palm cellulose-based ligand did not follow the Langmuir isotherm model pathway. This indicates that a single-layer adsorption did not occur on the palm cellulose-based poly(amidoxime) ligand.

Freundlich isotherm model

The Freundlich model is an empirical equation utilized for an assumption to the adsorption which occurs on the superficial of cellulose-based adsorbent and the energy of adsorptive is heterogeneous (Zheng et al. 2010). This model can be applied

Table 3 The nonlinear form of Langmuir isotherm parameters for the poly(amidoxime) adsorbent

Adsorbate	Langmuir		
	q_m (mg g^{-1})	K_L (L g^{-1})	R^2
Cu	256	0.110	0.999
Fe	229	0.179	0.999
Co	204	0.147	0.998
Pb	269	0.250	0.996
Ni	199	0.158	0.991

Table 4 The linear form of Langmuir and Freundlich isotherm parameters for poly(amidoxime) adsorbent

Adsorbate	Langmuir			Freundlich		
	q_m (mg g^{-1})	K_L (L g^{-1})	R^2	$1/n$	K_F (L mg^{-1})	R^2
Cu	877	0.00010	0.906	1.13	0.194	0.990
Fe	584	0.00017	0.981	1.16	0.209	0.987
Co	465	0.00020	0.976	1.22	0.254	0.992
Pb	549	0.00026	0.996	1.25	0.408	0.993
Ni	471	0.00018	0.966	1.20	0.226	0.993

to the multiple-layer adsorption of a reversible heterogeneous surface (Pan et al. 2016). The Freundlich isotherm theory presumes that the molecule or atom will first bind to the stronger binding sites and the degree of site occupation enrichment will cause the binding strength to slowly reduce. The nonlinear Freundlich isotherm is shown in Eq. 7 (Pan et al. 2016; Chen et al. 2018; Jang et al. 2018).

$$q_e = K_F C_e^{1/n} \tag{7}$$

where q_e (mg/g) is described as the equilibrium adsorption capacity of metal ions on the cellulose-based adsorbent, C_e (mg/L) is the equilibrium concentration of toxic ions in aqueous solution, K_F is Freundlich's constant, and $1/n$ is the heterogeneity factor.

The linear multiple-layer model of adsorption on the heterogeneous surface (Freundlich isotherm) was also widely used to evaluate the specification of isotherm and suitable model for multilayer adsorption system. The linear Freundlich isotherm theory (multiple-layer model of adsorption on the heterogeneous surface) is described as in Eq. 8 (Pan et al. 2016).

$$\log q_e = \log K_F + \frac{\log C_e}{n} \tag{8}$$

The linear plot of the Freundlich model was proposed in the log of q_e versus C_e, and the result is presented in Fig. 11. The constant of Freundlich (K_F) and binding power (n) of Freundlich adsorption isotherms of designated metal ions were found in the plot, and the outcome is shown in Table 3. The calculated results obtained is best fitted with the Freundlich model due to the correlation of R^2 values are persistent and consistent, which is > 0.99 using the experimental data. The linearity of the plots for R^2 values are 0.990, 0.987, 0.992, 0.993, and 0.993 for the copper, iron, cobalt, lead, and nickel, respectively. Therefore, it can be concluded that the palm cellulose-supported adsorbent is undergoing multiple-layer adsorption systems when binding the selected metal ions. The linear multiple-layer model of adsorption by Freundlich isotherm is well adapted to the isotherm parameters and suitable for a multilayer adsorption system. Moreover, the cooperative adsorption also occurs because the outcome of calculated n is in the range of 0 to 1. All the calculated results obtained from the slope and are displayed in Table 4.

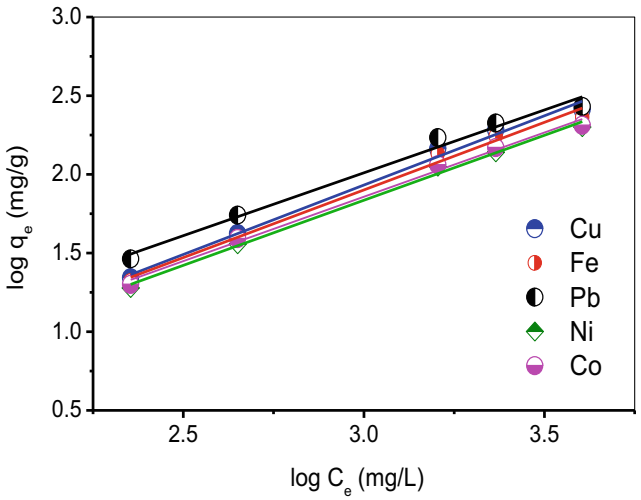

Fig. 11 Freundlich isotherm curves obtained by linear fitting on the adsorption of metal ions by the synthesized palm-based ligand; experimental variables were 0.5 g of poly(amidoxime), 15 mL distilled water, 5 mL pH 6 buffer solution, and 5 mL of 0.2 M synthetic metal ion solution and stirred for 2 h

Comparison of maximum adsorption capacities (q_m)

The maximum adsorption capacities (q_m) of the adsorbents, which were calculated by both the linear and nonlinear Langmuir model according to a reported method (Rahman et al. 2016a, b; Pan et al. 2018). It was observed that the q_m obtained from the nonlinear Langmuir model are very close to experimental values q_e. On the other hand, the q_m obtained by the linear Langmuir model is far different from all metal ions used in this study. The differences (D^a) between the q_m derived from nonlinear Langmuir model and the experimental data are presented in Table 5. Similarly, the differences (D^b) between the q_m derived from linear Langmuir model and the experimental data are also presented in Table 5. The results shown for this adsorption system of heavy metal ions are coordinated with amidoxime-functionalized ligand and the results derived from nonlinear fitting of the isotherm models are in good agreement (Table 5).

D^a differences between maximum adsorption capacities of nonlinear model and experimental data, D^b differences between the maximum adsorption capacities of linear model and experimental data

The goodness-of-fit for the linear form of Langmuir and Freundlich isotherm

In order to measure the goodness-of-fit for the two used isotherm models, hybrid error function (HYBRID) and Marquardt's percent standard deviation (MPSD) were determined by the following equation (Sanchooli et al. 2016):

$$\mathrm{HYBRID} = \frac{100}{N-P} \sum_{i=1}^{N} \left[\frac{\left(q_{e_i}^{exp} - q_{ei}^{cal} \right)^2}{q_{ei}^{exp}} \right] \tag{9}$$

$$\mathrm{MPSD} = 100 \sqrt{\frac{1}{N-P} \sum_{i=1}^{N} \frac{\left(q_{e_i}^{exp} - q_{ei}^{cal} \right)^2}{q_{ei}^{exp}}} \tag{10}$$

where $q_{e_i}^{exp}$ and q_{ei}^{cal} are the experimental equilibrium

Table 5 Comparison between the maximum adsorption capacities by the Langmuir nonlinear and linear isotherm models

Adsorbate	Exp. measured q_e (mg g^{-1})	Nonlinear Langmuir q_m (mg g^{-1})	Linear Langmuir q_m (mg g^{-1})	D^a (mg g^{-1})	D^b (mg g^{-1})
Cu	260	256	877	4	− 617
Fe	210	229	584	− 19	− 374
Co	168	204	465	− 36	− 297
Pb	272	269	549	3	− 277
Ni	172	199	471	− 27	− 299

adsorption capacity of metal ions on the cellulose-based adsorbent and the theoretical equilibrium adsorption capacity of metal ions on the cellulose-based adsorbent, respectively. N and P are the numbers of observations in the experimental isotherm and the number of parameters in the regression model.

In general, when values of error function are low, it means there is an agreement between the experimental and calculated data and the regression model converges and becomes favorable. The smaller HYBRID and MPSD values indicate a more accurate estimation of the q_e value. The HYBRID and MPSD parameters are listed in Table 6. The result is listed in Table 4 suggesting that Freundlich isotherm provides a better model of the sorption system compared to Langmuir (Sanchooli et al. 2016; Bopda et al. 2018).

Investigation of adsorption mechanism by XPS analysis

Amidoxime are the bidentate ligands which are efficiently bound with copper cations due to the strong chelating ability to transition metal cations. The X-ray photoelectron spectra (Scanning X-ray Microprobe PHI Quantera II) are acquired to explain the binding mechanisms of copper(II) on the poly(amidoxime) ligand. The wide-scan XPS spectra of polymer ligand binding with copper are shown in Fig. 12a and the pure form of poly(amidoxime) ligand is shown in Fig. 12b. For the wide scan, the binding energy (BE) peaks were found at 284.5, 399.6, and 531.2 eV corresponding to the C 1s, N 1s, and O 1s spectra, respectively. The binding of copper(II) is highlighted by the two new peaks with BEs of 932.7 and 952.0 eV for the signals of Cu2p3/2 and Cu2p1/2 as shown in Fig. 9a. However, in the core-level N 1s spectra for the polymer ligand, the N 1s peak of polymer ligand showed two peaks with BEs of 399.1 and 399.8 eV, which correspond to nitrogen atoms in NH_2–C and C=N–OH species, respectively. Binding with copper, a new peak for the N 1s was found with a BE of 400.8 eV owing to the coordinated bond of the amidoxime group with copper. This is due to the lone pair of electrons in the nitrogen atoms of the amidoxime group being donated to the metal atom of the Cu (Pan et al. 2016).

The O 1s XPS spectra of the polymer ligand also showed two peaks at the BEs of 531.0 and 531.9 eV, which correspond to the oxygen atoms in the C–OH and C=N–OH species, respectively. After binding with copper, a new peak at a BE of 532.4 eV belonging to the peaks of O 1s of the oxygen atoms in C=N–OH was formed. In principle, the XPS is a powerful tool to investigate the electron exchange between the donor and acceptor species. A lone pair of electrons in the nitrogen atom was donated to the copper metal resulting in the reduction of the electron density of the nitrogen atom, giving higher BE peaks. In the case of the O 1s core-level spectra, increased BE peaks during the sorption process due

Table 6 The analysis of error function between Langmuir and Freundlich isotherm parameters

Adsorbate	Langmuir		Freundlich	
	MPSD	HYBRID	MPSD	HYBRID
Cu	16.83	2.83	10.01	1.00
Fe	11.76	1.38	11.34	1.29
Co	10.05	1.01	9.15	0.84
Pb	10.82	1.17	9.30	0.86
Ni	10.58	1.12	9.57	0.92

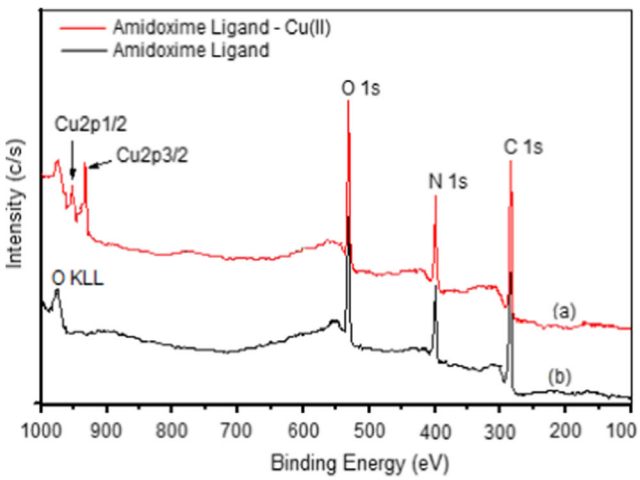

Fig. 12 Wide scan of the XPS of palm cellulose-based amidoxime ligand binding with copper (**a**) and palm-based amidoxime ligand (**b**)

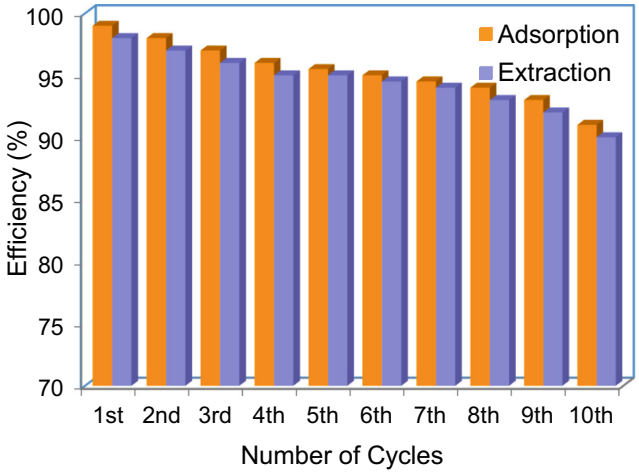

Fig. 13 Reusability studies of the polymeric ligand in several cycles of sorption/removal–extraction experiments

to the coordination between copper and amidoxime ligands can be observed.

Elution and reusability studies

The reusability of the adsorbent is the essential characteristic for practical applications. A series of the elution experiments were performed after the sorption test and the regeneration for reusability of the polymer adsorbent was examined. The copper metal ions may be liberated from the adsorbent in the acidic state. Therefore, complete extraction of the copper metals from the ligand was performed using 2 M of HCl solution for effective removal of the adsorbed copper ions from the ligands. The adsorbent can be regenerated into the initial configuration by washing several times with water after the elution experiments were performed. The reusability was investigated by the sorption/elution process for 10 cycles by using 150 mg of adsorbent (10 mL of 0.1 M copper solution for 2-h stirring period). Desorption experiments were carried out with 20 mL of 2 M HCl solution. The extraction efficiencies were decreased only about 10% after 10 cycles as shown in Fig. 13. Results show that the polymeric adsorbent can be reused for more than 10 cycles.

Electroplating wastewater purification

The poly(amidoxime) ligand was used to remove heavy metal ions from two different electroplating wastewaters. These wastewaters/spent liquors were obtained from the metal plating workshop (PCB etching) Porcel, Singapore. ICP analysis showed that wastewater 1 contained predominantly copper ions and wastewater 2 included both copper and iron ions. However, both samples also contained small quantities of other heavy metal ions including zinc, lead, chromium, nickel, cobalt, manganese, vanadium, and bismuth. The palm cellulose-based poly(amidoxime) ligand was successful at removing approximately 98% of copper and iron for both wastewaters. The ligand was slightly less efficient at removing zinc, nickel, and chromium waste with removal efficiencies of between 85 and 97% being achieved for both wastewaters. Table 7 outlines the removal efficiencies for each metal. Due to the nature of the ligand, it was significantly less efficient at removing calcium and magnesium. ICP-MS results show that the ligand eliminated more than 95% of copper, iron, lead,

Table 7 Metal content in electroplating wastewaters analyzed by ICP-MS

Metal ions	Wastewater 1			Wastewater 2		
	Before treatment (ppm)	After treatment (ppm)	Removal%	Before treatment (ppm)	After treatment (ppm)	Removal %
Cu	24.22	0.401	98.34	2.998	0.052	98.26
Fe	0.399	0.005	98.74	19.121	0.299	98.43
Zn	0.794	0.185	76.70	0.551	0.055	90.01
Pb	0.384	0.01	97.39	0.302	0.01	96.68
As	0.017	0.003	82.35	0.028	0.006	78.57
V	0.213	0.01	95.30	0.228	0.011	95.17
Co	0.216	0.01	95.37	0.268	0.013	95.14
Mg	0.602	0.529	12.12	0.852	0.629	26.17
Ca	1.852	1.685	9.01	1.621	1.431	11.72
Cr	0.435	0.011	97.47	0.569	0.017	97.01
Mn	0.322	0.011	96.58	0.302	0.015	95.03
Ni	5.978	0.141	97.64	0.897	0.126	85.95
Li	0.411	0.015	96.35	0.245	0.024	90.20
Sb	0.422	0.011	97.39	0.358	0.019	94.69

Table 8 Chemically modified grafted cellulose with various modifying agents/ligands functional groups, adsorbates, and their adsorption capacities for different adsorbents

Adsorbent supported materials	Modifying agents/ligands functional groups	Adsorbate	Adsorption capacity (mg g^{-1})	References
Cellulose	Glycidyl methacrylate (imidazole)	Cu(II)	70	O'Connell et al. 2006a, b, 2008
		Ni(II)	49	
		Pb(II)	85	
Cellulose	Amidoxime from acrylonitrile	Cu(II)	30	Kubota and Shigehisa 1995
Cellulose	Glycidyl methacrylate (GMA) onto titanium dioxide cellulose (TDC) followed by amination and ethylation reactions (amino)	Cr(VI)	123	Anirudhan et al. 2013
Cellulose	Acrylonitrile *N*,*N*-methylenebisacrylamide (amino)	Cd(II)	21	Zheng et al. 2010
Cellulose	Acrylic acid (carboxyl)	Cu(II)	328	Hajeeth et al. 2013
		Ni(II)	276	
Cellulose	Amidoxime from grafted kenaf cellulose	Cu(II)	326	Rahman et al. 2016a, b
		Fe(III)	273	
		Mn(II)	241	
		Cr(III)	228	
		Ni(II)	204	
Cellulose	Hydroxamic acid from grafted kenaf cellulose	Cu(II)	305	Rahman et al. 2017
		Co(II)	256	
		Cr(III)	254	
		Fe(III)	275	
		Ni(II)	198	
Cellulose	Amidoxime from grafted khaya cellulose	Cu(II)	282	Rahman et al. 2016a, b
		Fe(III)	254	
		Co(II)	221	
		Cr(III)	229	
		Ni(II)	202	
Cellulose	Amidoxime from grafted copolymers	Cu(II)	260	This study
		Fe(III)	210	
		Co(II)	168	
		Ni(II)	172	
		Pb(II)	272	

cobalt, nickel, and chromium from the wastewater samples. Results indicate that the synthesized polymeric ligand is a suitable adsorbent for the removal of metal ions from wastewater including spent liquor containing a high amount of copper and iron-like metal ions from PCB industry.

Comparison with other works

There is increasing awareness among the public regarding climate change and its adverse effects on biodiversity. To reduce the problem of environmental pollution, scientists have investigated using low-cost and natural biodegradable polymers such as cellulose, which can be modified to achieve elimination of metal ions and thereby aid in solving environmental problems. Functional groups such as carboxyl, amino, amine, or sulfur groups have a significant effect on the binding of metal ions on cellulose-based adsorbents and also affect the binding ability and the stability of the complex ligand (Liu et al. 2016). The acrylamide monomer can be grafted on the surface of cellulose and the resulting bio-ligand has COO–, $–NH_2$, and –OH functional groups that have shown efficient toxic metal extraction (Yousef et al. 2011).

To the best of our knowledge, chemical modification is the easiest way to modify the surface of the cellulose by directly attaching or grafting the selected monomer on the primary or secondary hydroxyl group (Rahman et al. 2016a, b, 2017). The intermediate product can then be subsequently functionalized with a known chelating ligand. The grafting of monomer on the surface of cellulose is a well-used method as the side chains covalently attached to the main chain of the cellulose backbone through ionic or free radical initiating processes (Pan et al. 2016). To create a highly reactive radical to initiate cellulose, ceric ammonia nitrate has been shown to be a powerful initiator that can provide highly efficient grafting (Rahman et al. 2016a, b).

The lone pair of electrons present on the nitrogen atom of amino groups can form covalent bonds with the metal ions. Amidoxime groups have a bidentate character which donates a proton and a basic lone pair of electrons on the nitrogen to coordinate with the metal ions. O'Connell et al.

have previouslysynthesized imidazole using a binding agent on a glycidyl methacrylate-grafted cellulose adsorbent O'Connell et al. 2006a, b). An important characteristic of imidazole is that the unsaturated nitrogen donors possesses a p-back bonding of the metal ions with imidazole generating a five-membered ring as a chelation process (O'Connell et al. 2006a, b, 2008). Several research groups reported on the modification of cellulose by radical grafting methods with various monomers and subsequent reactions generated by the potential adsorbents and binding metals ions such as copper, cadmium, chromium, and nickel (Kubota and Shigehisa 1995; Zheng et al. 2010; Hajeeth et al. 2013; Anirudhan et al. 2013). Table 8 shows the results of this study with respect to a previous work in the field.

Conclusions

Palm cellulose was extracted from empty fruit bunch (EFB) and was chemically modified with an acrylonitrile monomer and further functionalized into an amidoxime ligand. The developed material was for the extraction of metal ions from water and electroplated wastewater. The adsorption properties of palm fiber-supported amidoxime ligand were evaluated at different solution pH values, solution contact times, and metal ion concentrations. The palm cellulose, palm-based PAN, and poly(amidoxime) ligand were characterized by infrared spectroscopy, field emission scanning electron microscopy, and X-ray photoelectron spectroscopy. The binding performance of the ligand with various metal ions was examined individually at optimal pH. The binding capacity toward the selected metal ions was of the following order: $Pb^{2+} > Cu^{2+} > Fe^{3+} > Ni^{2+} > Co^{2+}$. The pseudo-first-order kinetic model fits the result when applied to heavy metal adsorption. The linear plot of Langmuir isotherm did not correlate with this model showing that the ligand does not undergo single-layer adsorption. Results showed a good fit to the Freundlich isotherm model with an R^2 value in excess of > 0.99. Hence, the binding of metal ions by palm-based amidoxime ligand occurs in a multilayer adsorption system. The good fit of Freundlich isotherm was further shown through the use of HYBRID and MPSD. Results showed that the Freundlich isotherm is more suitable to this experiment due to the lower value of HYBRID and MPSD error relative to Langmuir. The reusability of the ligand was assessed with results showing that the polymeric ligand can be reused for at least 10 cycles without any significant loss in ion removal capacity. The developed ligand is an efficient and effective candidate for heavy metal removal from electroplating wastewater.

Associated content The experimental part containing detailed preparation procedure and characterization is described.

Funding information This research work was supported by the Universiti Malaysia Sabah (SGI0061-2018).

References

Ahmad M, Ahmed S, Swami BL, Ikram S (2015) Adsorption of heavy metal ions: role of chitosan and cellulose for water treatment. Langmuir 79:109–155

Ahmadpour A, Eftekhari N, Ayati A (2014) Performance of MWCNTs and a low-cost adsorbent for chromium (VI) ion removal. J Nanostruct Chem 4(4):171–178

Anirudhan T, Nima J, Divya P (2013) Adsorption of chromium (VI) from aqueous solutions by glycidylmethacrylate-grafted-densified cellulose with quaternary ammonium groups. Appl Surf Sci 279:441–449

Arif N, Yadav V, Singh S, Singh S, Ahmad P, Mishra RK, Sharma S, Tripathi DK, Dubey NK, Chauhan DK (2016) Influence of high and low levels of plant-beneficial heavy metal ions on plant growth and development. Front Environ Sci 4:1–11

Ayawei N, Ebelegi AN, Wankasi D (2017) Modelling and interpretation of adsorption isotherms. J Chem 2017

Beccia MR, García B, García-Tojal J, Leal JM, Secco F, Tegoni M (2014) The mechanism of the Cu 2+[12-MC Cu (Alaha)-4] metallacrown formation and lanthanum (iii) encapsulation. Dalton Trans 43(24): 9271–9282

Bopda A, Tchuifon TDR, Nche GNA, Kamdem TA, Anagho SG (2018) Adsorption of 2,4-dinitrophenol on activated carbon prepared from cotton cakes: non linear isotherm modelling. Chem Sci Int J 24(1): 1–20

Chen X, Liu L, Luo Z, Shen J, Ni Q, Yao J (2018) Facile preparation of a cellulose-based bioadsorbent modified by hPEI in heterogeneous system for high-efficiency removal of multiple types of dyes. React Funct Polym 125:77–83

Donia AM, Yousif AM, Atia AA, Abd El-Latif HM (2014) Preparation and characterization of modified cellulose adsorbents with high surface area and high adsorption affinity for Hg (II). J Disper Sci Technol 35(3):380–389

dos Santos Silva L, de Oliveira Carvalho J, de Sousa Bezerra RD, da Silva M, Ferreira F, Osajima J, da Silva Filho E (2018) Potential of cellulose functionalized with carboxylic acid as biosorbent for the removal of cationic dyes in aqueous solution. Molecules 23(4):743

Dwivedi AD, Dubey SP, Hokkanen S, Fallah RN, Sillanpää (2014) Recovery of gold from aqueous solutions by taurine modified cellulose: an adsorptive–reduction pathway. Chem Eng J 255:97–106

Eigen M, Tamm K (1962) Sound absorption in electrolytes as a consequence of chemical relaxation. I. Relaxation theory of stepwise dissociation. Z. Elektrochem 66:107–121

Eigen M, Wilkins RG (1965) The kinetics and mechanism of formation of metal complexes. ACS Publications, Washington, D.C.

Fu J, Zhao C, Luo Y, Liu C, Kyzas GZ, Luo Y, Zhao D, An S, Zhu H (2014) Heavy metals in surface sediments of the Jialu River, China: their relations to environmental factors. J Hazard Mater 270:102–109

Furushima Y, Nakada M, Takahashi H, Ishikiriyama K (2014) Study of melting and crystallization behavior of polyacrylonitrile using ultrafast differential scanning calorimetry. Polymer 55(13):3075–3081

Hajeeth T, Vijayalakshmi K, Gomathi T, Sudha P (2013) Removal of Cu (II) and Ni (II) using cellulose extracted from sisal fiber and cellulose-g-acrylic acid copolymer. Int J Biol Macromol 62:59–65

Helm L, Merbach A (1999) Water exchange on metal ions: experiments and simulations. Coord Chem Rev 187(1):151–181

Hokkanen S, Bhatnagar A, Sillanpää M (2016) A review on modification methods to cellulose-based adsorbents to improve adsorption capacity. Water Res 91:156–173

Hong QL, Yong SQ, Jian X (2015) Microwave-assisted conversion of lignin. Biofuels Biorefineries 3:61–82

Jacob JM, Karthik C, Saratale RG, Kumar SS, Prabakar D, Kadirvelu K, Pugazhendhi A (2018) Biological approaches to tackle heavy metal pollution: a survey of literature. J Environ Manag 217:56–70

Jang HM, Yoo S, Choi YK, Park S, Kan E (2018) Adsorption isotherm, kinetic modeling and mechanism of tetracycline on Pinus taeda-derived activated biochar. Bioresour Technol 259:24–31

Ju A, Guang S, Xu H (2013) Effect of comonomer structure on the stabilization and spinnability of polyacrylonitrile copolymers. Carbon 54:323–335

Kiani GR, Sheikhloie H, Arsalani N (2011) Heavy metal ion removal from aqueous solutions by functionalized polyacrylonitrile. Desalination 269:266–270

Kubota H, Shigehisa Y (1995) Introduction of amidoxime groups into cellulose and its ability to adsorb metal ions. J Appl Polym Sci 56(2):147–151

Lin G, Wang S, Zhang L, Hu T, Peng J, Cheng S, Fu L, Srinivasakannan C (2018) Selective recovery of Au (III) from aqueous solutions using 2-aminothiazole functionalized corn bract as low-cost bioadsorbent. J Clea Prod 196:1007–1015

Liu L, Xie JP, Li YJ, Zhang Q, Yao JM (2016) Three-dimensional macroporous cellulose-based bioadsorbents for efficient removal of nickel ions from aqueous solution. Cellulose 23(1):723–736

Long H, Zhao Z, Chai Y, Li X, Hua Z, Xiao Y, Yang Y (2015) Binding mechanism of the amidoxime functional group on chelating resins toward gallium (III) in Bayer liquor. Ind Eng Chem Res 54(33): 8025–8030

Lutfor MR, Silong S, Md Zin W, Ab. Rahman MZ, Ahmad M, Haron J (2000) Preparation and characterization of poly(amidoxime) chelating resin from polyacrylonitrile grafted sago starch. Eur Polymer J 36(10):2105–2113

O'Connell DW, Birkinshaw C, O'Dwyer TF (2006a) A modified cellulose adsorbent for the removal of nickel (II) from aqueous solutions. J Chem Technol Biotechnol 81(11):1820–1828

O'Connell D, Birkinshaw C, O'Dwyer T (2006b) A chelating cellulose adsorbent for the removal of Cu (II) from aqueous solutions. J Appl Polym Sci 99(6):2888–2897

O'Connell DW, Birkinshaw C, O'Dwyer TF (2008) Heavy metal adsorbents prepared from the modification of cellulose: a review. Bioresour Technol 99(15):6709–6724

Pan Y, Wang F, Wei T, Zhang C, Xiao H (2016) Hydrophobic modification of bagasse cellulose fibers with cationic latex: adsorption kinetics and mechanism. Chem Eng J 302:33–43

Pan Y, Shi X, Cai P, Guo T, Tong Z, Xiao H (2018) Dye removal from single and binary systems using gel-like bioadsorbent based on functional-modified cellulose. Cellulose 25(4):2559–2575

Rahman ML, Sarkar SM, Yusoff MM, Abdullah MH (2016a) Efficient removal of transition metal ions using poly (amidoxime) ligand from polymer grafted kenaf cellulose. RSC Adv 6(1):745–757

Rahman ML, Sarkar SM, Yusoff MM, Kulkarni AKD, Chowdhury ZZ, Ali ME (2016b) Poly(amidoxime) from polymer-grafted khaya cellulose: an excellent medium for the removal of transition metal cations from aqueous solution. Bioresources 11(3):6780–6800

Rahman ML, Sarkar SM, Yusoff MM, Abdullah MH (2017) Optical detection and efficient removal of transition metal ions from water using poly (hydroxamic acid) ligand. Sensor Actuat B Chem 242: 595–608

Robson FR, Luiz CP, Nilton PA, Carlos ARBJ (2014) Synthesis and thermal behavior of polyacrylonitrile/vinylidene chloride copolymer. Polimeros 24(3):259–268

Robson FR, Luiz CP, Nilton PA, Carlos ARBJ (2015) Thermal stabilization study of polyacrylonitrile fiber obtained by extrusion. Polimeros 25(6):523–530

Salah M, El-Bahy ZM, El-Bahy (2015) Synthesis and characterization of polyamidoxime chelating resin for adsorption of Cu (II), Mn(II) and Ni(II) by batch and column study. J Envriron Chen Eng 4(1):276–286

Sanchooli MM, Rahdar S, Tanghavi M (2016) Cadmium removal from aqueous solutions using saxaul tree ash. Iran J Chem Eng 35(3):45–52

Silva SM, Sampaio KA, Ceriani R, Verhé R, Stevens C, De Greyt W, Meirelles AJ (2013) Adsorption of carotenes and phosphorus from palm oil onto acid activated bleaching earth: equilibrium, kinetics and thermodynamics. J Food Eng 118(4):341–349

Wani AL, Anjum A, Jawed AU (2015) Lead toxicity: a review. Interdiscip Toxicol 8(2):55–64

Wilkins R (1964) The kinetics of formation of some divalent transition metal-dye complexes, studied by the temperature-jump relaxation method. Inorg Chem 3(4):520–522

Wu W, Wu P, Yang F, Sun DI, Zhang DX, Zhou YK (2018) Assessment of heavy metal pollution and human health risks in urban soils around an electronics manufacturing facility. Sci Total Environ 630:53–61

Yousef RI, El-Eswed B, Ala'a H (2011) Adsorption characteristics of natural zeolites as solid adsorbents for phenol removal from aqueous solutions: kinetics, mechanism, and thermodynamics studies. Chem Eng J 171(3):1143–1149

Zheng L, Dang Z, Yi X, Zhang H (2010) Equilibrium and kinetic studies of adsorption of Cd (II) from aqueous solution using modified corn stalk. J Hazard Mater 176(1–3):650–656